Lattice dynamical and thermodynamical properties of ReB_2, RuB_2, and OsB_2 compounds in the ReB_2 structure

E. Deligoz[a)†], K. Colakoglu[b)], and Y. O. Ciftci[b)]

[a)] *Department of Physics, Aksaray University,* 68100, *Aksaray, Turkey*

[b)] *Department of Physics, Gazi University, Teknikokullar,* 06500, *Ankara, Turkey*

(Received 2 January 2012; revised manuscript received 21 May 2012)

Structural and lattice dynamical properties of ReB_2, RuB_2, and OsB_2 in the ReB_2 structure are studied in the framework of density functional theory within the generalized gradient approximation. The present results show that these compounds are dynamically stable for the considered structure. The temperature-dependent behaviors of thermodynamical properties such as internal energy, free energy, entropy, and heat capacity are also presented. The obtained results are in good agreement with the available experimental and theoretical data.

Keywords: *ab initio* calculations, lattice dynamical properties, thermodynamical properties, diborides

PACS: 63.20.D–, 71.15.Nc, 65.40.Ba **DOI:** 10.1088/1674-1056/21/10/106301

1. Introduction

With superior properties of higher compressional strength, thermal conductivity, refractive index, and chemical stability, as well as higher hardness, hard materials have been widely used in industry.[1] Unfortunately, almost all superhard materials (diamond, cubic BN, etc.) are expensive because they either occur naturally in limited supplies or have to be made at high pressure synthetically.[2] Therefore, intense research efforts have been made to design new ultrahard materials.[1−4] A promising approach to designing superhard materials is to combine transition metals, each possessing a high bulk modulus with small, covalent bond forming atoms such as boron, carbon, nitrogen or oxygen.[2,5]

Many theoretical and experimental studies have been carried out on the structural, elastic, mechanical,[1−3,6−30] electronic, and phonon properties of XB_2 (X=Re, Ru, and Os) in ReB_2 structures. Most of the theoretical calculations for these compounds have been made by using the density functional theory within the generalized gradient approximation (GGA) and the local density approximation (LDA). Structural, elastic, and mechanical properties[1−3,6−10,12−14,16−18,21−30] of ReB_2, RuB_2, and OsB_2 have been investigated through considerable experimental and theoretical work. The results of some of these studies indicated that ReB_2 is a superhard material[3,5,10,12,20] and RuB_2, OsB_2 are hard materials.[1,3,5,25] These compounds are also ultraincompressible materials.[5,14,19,23,27] The electronic and thermodynamic properties[2,11,14−17,19−22,27,29] of these compounds have also been investigated under high pressure and temperature. However, relatively little attention has been paid to the lattice dynamical properties of ReB_2 and OsB_2 in the ReB_2 structure.[2,28]

To the best of our knowledge, the lattice dynamical properties of RuB_2 in the ReB_2 structure have not been investigated by using any theoretical or experimental method. Consequently, the main purpose of this work is to provide some additional information to the existing data for ReB_2, RuB_2, and OsB_2 compounds by using *ab initio* total energy calculations. We calculate and analyse thermodynamical properties such as internal energy, free energy, entropy, and heat capacity of these compounds for the first time. The method of calculation is given in Section 2; the results are discussed in Section 3. Finally, the summary and conclusion are presented in Section 4.

2. Method of calculation

The present calculations are based on the density functional formalism and generalized gradient approx-

†Corresponding author. E-mail: edeligoz@yahoo.com

© 2012 Chinese Physical Society and IOP Publishing Ltd

imation (GGA) using the Perdew–Burke–Ernzerhof (PBE) functional[31] for the exchange–correlation energy in the Siesta code.[32,33] This code calculates the total energies and atomic forces using a linear combination of atomic orbitals as the basis set. The basis set is based on the finite-range pseudoatomic orbitals (PAOs) of the Sankey–Niklewsky type,[34] and generalized to include multiple-zeta decays. The interactions between electrons and core ions are simulated with the separable Troullier–Martins[35] norm-conserving pseudopotentials.

Atomic pseudopotentials are generated separately for atoms Ru, Re, Os, and B by using the $5s^1 5p^0 4d^7$, $6s^2 6p^0 5d^5$, $6s^2\ 6p^0 5d^6$, and $2s^2\ 2p^1$ atomic configurations, respectively. The cut-off radii for the present atomic pseudopotentials are taken to be 2.70 a.u. (1 a.u.=1 atomic unit) for s channel, 2.77 a.u. for p channel, 2.51 a.u. for d channel, and 2.51 a.u. for f channel of Re; 2.56 a.u. for s channel, 2.69 a.u. for p channel, 2.50 a.u. for d channel, and 2.50 a.u. for f channel of Ru;, 2.67 a.u. for s channel, 2.81 a.u. for p channel, 2.60 a.u. for d channel, 2.60 a.u. for f channel of Os, and 1.74 a.u. for the s, p, d, and f channel of B.

Atoms are allowed to relax until atomic forces are less than 0.005 eV·Å^{-1} (1 Å=0.1 nm). The cut-off energy is taken to be 400 Ry. 455 k-points are found to be adequate to obtain the total energy to an accuracy of 1 meV/atom for ReB_2, RuB_2, and OsB_2 within the ReB_2 structure.

The phonon dispersion curves and phonon density of states are calculated with the direct method[36] as implemented in the phonon software[36,37] in a manner similar to that in our recent work.[38−42] The optimized rhombohedral supercell with 36 atoms and basis vectors are given as $\boldsymbol{a}_\mathrm{s} = 2a + c$, $\boldsymbol{b}_\mathrm{s} = 2b + c$, $\boldsymbol{c}_\mathrm{s} = -2a-2b+c$, where $\boldsymbol{a}$, $\boldsymbol{b}$, $\boldsymbol{c}$ are the primitive translation vectors of the hexagonal unit cell.[43] The symmetry of the selected rhombohedral supercell breaks the two-fold symmetry axis, and lowers the $P6/mmm$ space group to $R3m$. Here, the displacement amplitudes are taken to be 0.03 Å. This value is sufficient to attain the desired accuracy and to fulfill the conditions (the translational–rotational invariance laws) of the harmonic approximation.

The positive and negative atomic displacements along x, y, and z axes are also taken into account. The force constants and dynamical matrices are obtained from the Hellmann–Feynman forces calculated with small individual displacements of nonequivalent atoms.

As is well known, the thermodynamic properties of the crystals can be determined in detail by phonons. The approach to finding the scaling factor between pressure and temperature, which is the essence of the harmonic approximation, is given below.

The Gibbs free energy $G(T, P)$ is defined as

$$G(T, P) = F(T, V) + PV, \tag{1}$$

where $F(T, V)$ is the free energy of the crystal. It consists of two contributions and is expressed as follows:

$$F(T, V) = E(V) + F_\mathrm{ph}(T, V), \tag{2}$$

where $E(V)$ denotes the ground state energy and $F_\mathrm{ph}(T, V)$ is the phonon free energy at a given unit cell volume V. The temperature T appears in $F_\mathrm{ph}(T, V)$ via the phonon term. The more explicit forms of the internal energy, free energy, entropy, and heat capacity in the harmonic approximation per primitive unit cell are given[37] as follows:

$$E = \frac{1}{2} r \int_0^\infty g(\omega)(\hbar\omega) \coth\left(\frac{\hbar\omega}{2k_\mathrm{B}T}\right) \mathrm{d}\omega, \tag{3}$$

$$F = rk_\mathrm{B}T \int_0^\infty g(\omega) \ln\left[2\sinh\left(\frac{\hbar\omega}{2k_\mathrm{B}T}\right)\right] \mathrm{d}\omega, \tag{4}$$

$$S = rk_\mathrm{B} \int_0^\infty g(\omega) \left\{ \left(\frac{\hbar\omega}{2k_\mathrm{B}T}\right) \left[\coth\left(\frac{\hbar\omega}{2k_\mathrm{B}T}\right) - 1\right] - \ln\left[1 - \exp\left(\frac{\hbar\omega}{2k_\mathrm{B}T}\right)\right] \right\} \mathrm{d}\omega, \tag{5}$$

$$C = rk_\mathrm{B} \int_0^\infty g(\omega) \left(\frac{\hbar\omega}{k_\mathrm{B}T}\right)^2 \times \frac{\exp(\hbar\omega/k_\mathrm{B}T)}{[\exp(\hbar\omega/k_\mathrm{B}T) - 1]^2} \mathrm{d}\omega, \tag{6}$$

where r is the number of degrees of freedom in a unit cell, $\hbar$ is the Planck constant, k_B is the Boltzmann constant, T is the temperature, and $g(\omega)$ is the phonon density of states.

3. Results and discussion

3.1. Structural properties

For the ReB_2-type structure, the two transition metal atoms occupy sites (1/3, 2/3, 1/4) and (2/3, 1/3, 3/4) while the four boron atoms occupy sites (2/3, 1/3, z), (1/3, 2/3, 1/2 + z), (2/3, 1/3, 1/2 − z), (1/3, 2/3, 1 − z). We first optimize the lattice parameters to obtain a relaxed structure. The initial lattice parameters are taken from previous work as a starting point for geometry optimization. The calculated lattice and internal parameters are listed in Table 1 along with the results available from other work for comparison. It can be seen that the present results are in good agreement with the theoretical values.

Table 1. Calculated equilibrium lattice parameters (a, c in Å) and internal parameters (z) along with those available from other work for ReB_2, RuB_2, and OsB_2 in the ReB_2 structure.

Materials	Reference	a/Å	c/Å	c/a	z
ReB_2	present (GGA-PBE)	2.875	7.421	2.581	0.0476
	theory[12] (GGA-PBE)	2.901	7.478	2.578	0.0478
	theory[11] (GGA-USPP)	2.901	7.479	2.578	0.048
	theory[12] (GGA-PPE)	2.880	7.420	2.576	
	theory[[13] (GGA-PBE)	2.881	7.409	2.572	
	theory[17] (GGA-PAW)	2.913	7.506	2.577	
	theory[20] (GGA-PAW)	2.92	7.515	2.573	
	experimental[6]	2.900	7.478	2.579	0.048
	experimental[9]	2.899	7.473	2.578	
	experimental[18]	2.900	7.477	2.578	
RuB_2	present (GGA-PBE)	2.917	7.242	2.482	0.0488
	theory[25] (GGA-PBE)	2.916	7.264	2.491	
	theory[29] (GGA-PBE)	2.91	7.275	2.500	
OsB_2	present (GGA-PBE)	2.940	7.332	2.494	0.0515
	theory[28] (GGA)	2.941	7.338	2.495	

3.2. Phonon properties

The phonon dispersion curve provides important information about the dynamical properties of materials. Many physical properties of solids depend on their phonon properties, such as specific heat, thermal expansion, free energy, heat conduction, sound velocity, and electron–phonon coupling. In addition, low frequency modes can be associated with phase transformations, while imaginary frequencies show that the calculated structure is not the most stable one.

The obtained phonon dispersion curves and the corresponding phonon density of states for ReB_2, RuB_2, and OsB_2 in a ReB_2-type structure along the high-symmetry directions are illustrated in Fig. 1. It can be seen that ReB_2, RuB_2, and OsB_2 compounds possess very similar dispersion curves and the corresponding density of states. The unit cell of a ReB_2-type structure contains six atoms, which gives rise to a total of 18 phonon branches, which contain three acoustic modes and 15 optical modes.

The calculated phonon dispersion curves do not contain a soft mode at any wave vector, and there are no optical phonon branches with dispersions that dip toward the zero frequency. This confirms that these compounds are dynamically stable. The phonon dispersion curves of these compounds exhibit two quite separate bands: the low frequency region (below about 8 THz, which contains acoustic and lowest frequency optical bands) and the high frequency region (above about 13 THz, which contains high-frequency optical bands).

The three lowest frequency optical modes are dominated by the transition metal atoms displacement while the high-frequency optical modes are dominated by the lighter B atom displacement. The high-frequency phonon modes (about 22 THz, 23 THz, and 24 THz for OsB_2, RuB_2, and ReB_2 compounds, respectively) are less dispersive than the other optical phonon branches. Therefore, there is a very sharp peak at each of these frequencies in the DOS for these compounds. We can also see that the phonon dispersion curve is degenerate at A point.

The maximum value of the phonon frequencies for optical branches follows the order from larger to smaller as ReB_2 (25.595 THz at M point) $\rightarrow$ RuB_2 (24.485 THz at H point) $\rightarrow$ OsB_2 (22.776 THz at K point). The highest frequency is not at the Γ point. A similar characteristic of the highest frequency is not observed at the Γ point in many transition metal carbides, nitrides, and borides.[44,45] This characteristic can be explained by differences in their total and reduced masses as well as their lattice constants. The magnitude of the band gap follows the order of OsB_2 (6.046 THz) $\rightarrow$ ReB_2 (4.833 THz) $\rightarrow$ RuB_2 (3.217 THz). In Fig. 1, there are nearly flat bands along Γ–M and Γ–A directions, which signals strong stiffness, bringing about a very high bulk modulus for these compounds.[44]

As shown in Fig. 1, there are a few optical phonon modes at the bottom of the optical phonon branch moving down toward the acoustic region along the Γ–M–A directions. This interaction will lead to the heat-carrying acoustic modes be-

ing scattered by low-frequency optical modes, which can also reduce the phonon velocity and hence thermal conductivity.[46] So, the low-lying optical phonon mode plays a very important role in lowering the thermal conductivity.[47] Some optical modes are weakly dispersive, and these flat optical branches contribute little to heat transport.[46,47] The acoustic branches have steep slopes, indicating large elastic coefficients.

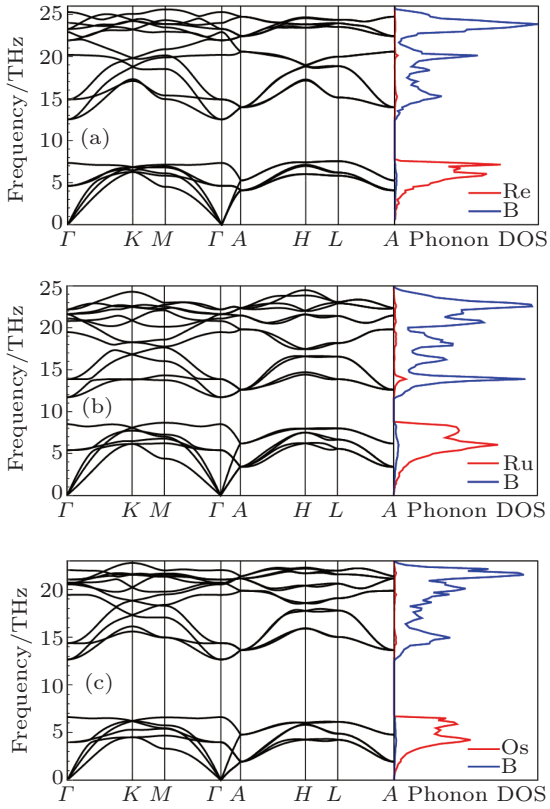


Fig. 1. (colour online) Calculated phonon dispersions, total and partial density of states (a) ReB_2, (b) RuB_2, and (c) OsB_2.

On the right side of each of the phonon dispersion curves, the corresponding partial density of phonon states is also plotted (see Fig. 1) for all compounds. From the partial density of states of each displaced atom and the polarization vector analysis, it is seen that the lower frequency region (about < 8 THz) is dominated by the displacements of transition metal (TM) atoms while the higher frequency region (about > 13 THz) is dominated by the displacements of boron atoms, i.e., partial density of state (PDOS) profiles with similar features show that in the lower-frequency region B atom vibrates with a very small amplitude, but in the higher-frequency region transition metal atoms vibrate each with a very small amplitude. The covalent character of the B–B bonding is also decisive for the high frequency of phonons involving the boron atoms.

The zone centre phonon modes are of special interest in the lattice dynamics of solids. All of the gamma-point modes involve atomic vibrations along the directions of x, y, and z. For the ReB_2-type structure, optic modes have the following irreducible representations:[2]

$$\Gamma = A_{1g} + 2A_{2u}(\mathrm{IR}) + 2B_{1g} + B_{2u} + E_{2u} + 2E_{2g}(\mathrm{R}) + 2E_{1u}(\mathrm{IR}) + E_{1g}(\mathrm{R}).$$

Here, the Raman active modes are labeled by R and infrared active by IR while the silent modes are unmarked. The crystal symmetry implies six Raman- and six IR-active modes. The calculated various phonon frequencies are listed in Table 2 along with the theoretical ones for comparison. $2E_{2u}$, $2E_{1u}$, A_{2u}, $2E_{1g}$, B_{2u}, $2E_{2g}$, B_{1g}, and A_{1g} modes are dominated by the atomic vibrations of boron atoms in the higher-frequency region while the $2E_{2g}$ (in a–b plane) and B_{1g} (along c axis) modes are dominated by the atomic vibrations of transition metal atoms (Re, Ru, and Os) in the lower-frequency region for all compounds. These results are consistent with those obtained for ReB_2 in Ref. [2]. Unfortunately, there are no theoretical and experimental data available to compare with those of OsB_2 and RuB_2 compounds. Generally, one can see that ReB_2 compound has higher phonon energies than the RuB_2 and OsB_2 compounds. Hence, the ReB_2 compound favours heat dissipation, and therefore a higher thermal conductivity is expected.[48]

Table 2. Calculated phonon energies (in THz) along with those available from other work of ReB_2, RuB_2, and OsB_2 at Γ point.

	Species									
Materials	$2E_{2g}$	B_{1g}	$2E_{2u}$	$2E_{1u}$	A_{2u}	$2E_{1g}$	B_{2u}	$2E_{2g}$	B_{1g}	A_{1g}
ReB_2	4.624	7.330	12.163	14.746	20.135	21.793	22.875	23.167	23.930	25.247
Theory[a]	4.497	6.892	12.114	14.411	18.884	20.601	21.181	21.858	22.031	23.624
RuB_2	5.395	8.501	11.718	13.875	19.480	20.802	21.098	21.608	21.633	22.189
OsB_2	3.997	6.614	12.660	14.370	19.431	20.529	20.622	20.727	21.040	22.021

[a]Ref. [2] (GGA-PBE)

It is known from Refs. [49]–[52] that the difference in bond length between the transition metal (TM)–B, TM–TM (in-plane), and TM–TM (out-of-plane) stems from the species difference of the TM atoms in crystal and influences the electronic properties, vibrational behavior, electron–phonon coupling, etc. As expected, in our case the computed gamma-point frequencies of these materials in Fig. 1 are not equal to each other, owing to the different reduced mass, bond length, and lattice constants.

3.3. Temperature dependence of thermodynamic quantities

Equations (3)–(6) are used to plot the temperature dependences of internal energy (E), free energy (F), entropy (S), and heat capacity (C) at constant volume for each compound, by using the data obtained from Siesta and Phonon software. The temperature-dependent variations of the free energy, internal energy, entropy, and heat capacity at constant volume are plotted in Fig. 2 for RuB_2, ReB_2, and OsB_2. These predicted high temperature behaviors could give some information when these compounds are annealed at different temperatures to improve their performances. The temperature variations of thermodynamical functions for these compounds show usual trends due to their similar vibrational properties. Unfortunately, there are no experimental and theoretical data available for comparison with our results.

The calculated internal energies for ReB_2, RuB_2, and OsB_2 in the ReB_2 structure each as a function of temperature are displayed in Fig. 2. The results suggest that above 300 K, the internal energies increase almost linearly with temperature. However at temperature below 300 K there are three separate groups, the difference between the groups decreases with temperature. This may be due to the contribution from higher frequencies resulting from lighter boron atom vibrations.[53] The total and partial (not shown here in the figure) internal energy graphs exhibit a similar trend for these compounds and the contributions to internal energy from B are dominant over those from transition metal atoms. At high temperatures the internal energy tends to display k_BT behavior.

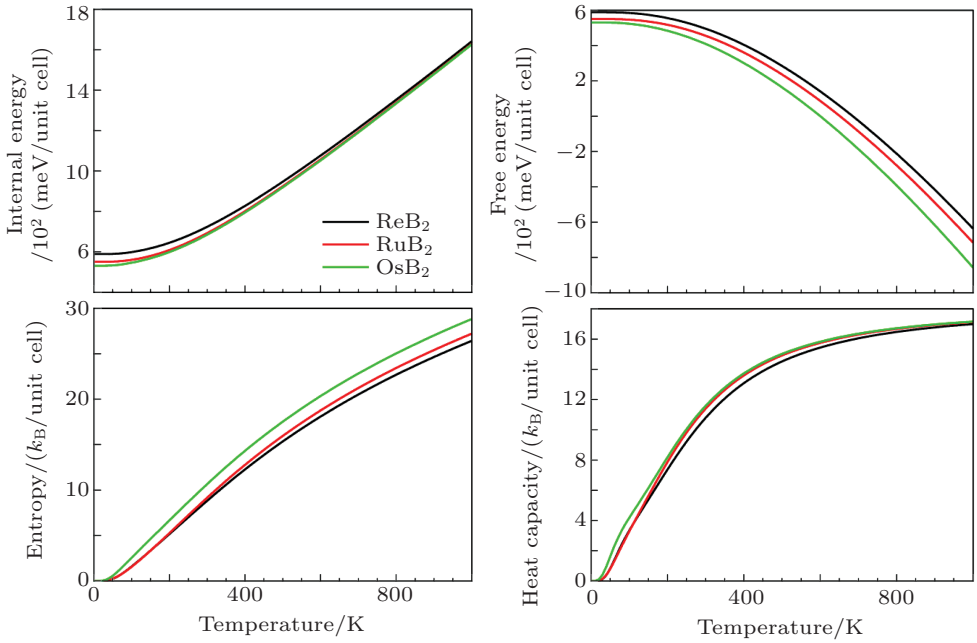


Fig. 2. (colour online) Temperature dependences of internal energy, free energy, entropy, and heat capacity for ReB_2, RuB_2, and OsB_2.

Figure 2 also shows the variations of the free energy at various temperatures for the same compounds. Overall profiles of all the plots show similar characteristics and free energy decrease gradually with temperature increasing. This behavior is due to the fact that both vibrational internal energy (E) and entropy (S) increase with temperature increasing, thereby leading to the decrease in free energy.[54] From the study of free energy, we conclude that these compounds are thermodynamically stable below 1000 K. The free and

internal energy at zero temperature represent the zero-point motion and the calculated values are 586.72, 549.73, and 530.95 meV/unit cell for ReB_2, RuB_2, and OsB_2, respectively. Obviously, one can see that the ReB_2 compound has higher free and internal energy compared with RuB_2 and OsB_2 compounds. Free energy calculation demonstrates that OsB_2 is thermodynamically more stable than ReB_2 and RuB_2.

The variations of entropy with temperature for ReB_2, RuB_2, and OsB_2 are given in Fig. 2 for the same temperature range. Obviously, at 0 K, their entropies are zero and the entropy changes increase rapidly as temperature increases at low temperature, while the variations of entropy are small above about 500 K. As the temperature increases the vibrational contribution to the entropy increases, therefore the entropy increases with temperature increasing.[54] The calculated values of enthalpy at room temperature are 8.982, 9.307, and 10.783 k_B/unit cell for ReB_2, RuB_2, and OsB_2, respectively. Their differences are due to the larger contribution from the low phonon frequency in OsB_2 than that in ReB_2, and RuB_2.[55] The low-frequency modes have longer wavelengths, which are associated with larger volumes in the configurational space. Therefore, they cause higher values for specific heat and entropy.[56] From Fig. 2, one can see that at low-temperature (about < 300 K) ReB_2 has higher entropy than RuB_2 compound. However, an opposite situation occurs when the temperature increases (about > 300 K): its entropy is lower than that of RuB_2 compound. The total and partial (not shown in the figure) entropy graphs each exhibit a similar trend and the contributions to entropy from transition metal atoms are dominant over them from boron atoms.

The contributions to the total heat capacity from the lattice vibrations of ReB_2, RuB_2, and OsB_2 are illustrated in Fig. 2. Figure 2 implies that while the temperature is about $T < 700$ K, C_v increases very rapidly with temperature increasing; when the temperature is about $T > 700$ K, C_v increases slowly with temperature increasing and it almost approaches to a constant called the Dulong–Petit limit. The Debye T^3 law is obeyed at lower temperature for all borides. At high temperature, C_v approaches to approximately 16.90, 17.01, and 17.121 k_B/unit cell for ReB_2, RuB_2, and OsB_2, respectively. Moreover, the variation of heat capacity is similar to that of entropy. In a broad temperature range, a RuB_2 compound has a larger heat capacity than OsB_2 and ReB_2 compounds. The temperature is limited to 1000 K to minimize the potential influence of anharmonicity in all graphs.

4. Summary and conclusion

The presented results on the structural, vibrational, and thermodynamic properties for ReB_2, RuB_2, and OsB_2 in ReB_2 structure are obtained using the first-principles calculations implemented in Siesta within the GGA approximation. Our lattice parameters are in agreement with the available experimental and theoretical ones. The original aspects of the present calculations are concerned with the phonon dispersion curves and thermodynamical results at various temperatures. The calculated phonon dispersion curves do not contain a soft mode at any wave vector, which confirms the dynamical stability of ReB_2, RuB_2, and OsB_2 in the ReB_2 structure. The temperature dependences of the internal energy, free energy, entropy, and heat capacity for these compounds are also calculated. The internal energy, entropy, and specific heat increase with temperature increasing while the Gibbs free energies decrease with temperature increasing for all the three compounds. Consequently, we conclude that our theoretical predictions on the considered properties of the present compounds will be helpful for further experimental and theoretical investigations in the future.

References

[1] Ren F Z, Wang Y X and Zhang G B 2009 *Chin. Phys. Lett.* **26** 016102

[2] Zhou W, Wu H and Yildirim T 2007 *Phys. Rev.* B **76** 184113

[3] Simunek A 2009 *Phys. Rev.* B **80** 060103(R)

[4] Kaner R B, Gilman J J and Tolbert S H 2005 *Mater. Sci.* **308** 1268

[5] Chung H Y, Weinberger M B, Yang J, Tolbert S H and Kaner R B 2008 *Appl. Phys. Lett.* **92** 261904

[6] Chung H Y, Weinberger M B, Levine J B, Kavner A, Yang J M, Tolbert S H and Kaner R B 2007 *Science* **316** 436

[7] Koehler M R, Keppens V, Sales B C, Jin R and Mandrus D 2009 *J. Phys.* D: *Appl. Phys.* **42** 095414

[8] Qin J, He D, Wang J, Fang L, Lei L, Li Y, Hu J, Kou Z and Bi Y 2008 *Adv. Mater.* **20** 4780

[9] Pellicer-Porres J, Segura A, Muñoz A, Polian A and Congeduti A 2010 *J. Phys.: Condens. Matter* **22** 045701

[10] Otani S, Korsukova M M and Aizawa T 2009 *J. Alloy Compd.* **47** L28

[11] Peng F, Liu Q, Fu H and Yang X 2009 *Solid State Comm.* **149** 56

[12] Aydin S and Simsek M 2009 *Phys. Rev.* B **80** 134107

[13] Hao X, Xu Y, Wu Z, Zhou D, Liu X, Cao X and Meng J 2006 *Phys. Rev.* B **74** 224112

[14] Liang Y C and Zhang B 2007 *Phys. Rev.* B **76** 132101

[15] Li Y L, Zhong G H and Zhi Z 2009 *Chin. Phys.* B **18** 4437

[16] Zhang R F, Veprek S and Argon A S 2007 *Appl. Phys. Lett.* **91** 201914

[17] Wang Y X 2007 *Appl. Phys. Lett.* **91** 101904
[18] Frotscher M, Hölzel M, Albert B and Anorg Z 2010 *Allg. Chem.* **636** 1783
[19] Chen X Q, Fu C L, Krcmar M and Painter G S 2008 *Phys. Rev. Lett.* **100** 196403
[20] Zhang R F, Legut D, Niewa R, Argon A S and Veprek S 2010 *Phys. Rev.* B **82** 104104
[21] Zhua X, Li D and Cheng X 2008 *Solid State Comm.* **147** 301
[22] Peng F, Peng W, Fu H and Yang X 2009 *Physica* B **404** 3363
[23] Chung H Y, Weinberger M B, Yang J M, Tolbert S H and Kaner R B 2008 *Appl. Phys. Lett.* **92** 261904
[24] Yang J W, Chen X R, Luo F and Ji G F 2009 *Physica* B **404** 3608
[25] Kanoun M B, Shein I R and Goumri-Said S 2010 *Solid State Comm.* **150** 1095
[26] Lazar P, Chen X Q and Podloucky R 2009 *Phys. Rev.* B **80** 012103
[27] Gou H, Hou L, Zhang J, Li H, Sun G and Gao F 2006 *Appl. Phys. Lett.* **88** 221904
[28] Ren F, Wang Y and Lo V C 2010 *J. Solid State Chem.* **183** 915
[29] Luo F, Cheng Y, Ji G F and Chen X R 2009 *Chin. Phys. Lett.* **26** 097101
[30] Tu Y and Wang Y 2011 *Solid State Comm.* **151** 238
[31] Perdew J P, Burke K and Ernzerhof M 1996 *Phys. Rev. Lett.* **77** 3865
[32] Ordejón P, Artacho E and Soler J M 1996 *Phys. Rev.* B **53** R10441
[33] Soler J M, Artacho E, Gale J D, García A, Junquera J, Ordejón P and Sánchez-Portal D 2002 *J. Phys.: Condens. Matter* **14** 2745
[34] Sankey O F and Niklewski D J 1989 *Phys. Rev.* B **40** 3979
[35] Troullier N and Martins J L 1991 *Phys. Rev.* B **43** 1993
[36] Parlinski K, Li Z Q and Kawazoe Y 1997 *Phys. Rev. Lett.* **78** 4063
[37] Parlinski K 2010 Software PHONON
[38] Deligoz E, Colakoglu K and Ciftci Y O 2009 *Solid State Comm.* **149** 1843
[39] Deligoz E, Colakoglu K and Ciftci Y O 2010 *Solid State Comm.* **150** 405
[40] Deligoz E, Colakoglu K and Ciftci Y O 2010 *Comp. Mater. Sci.* **47** 875
[41] Ozisik H, Deligoz E, Colakoglu K and Ciftci Y O 2011 *Comp. Mater. Sci.* **50** 1057
[42] Deligoz E, Ozisik H, Colakoglu K, Surucu G and Ciftci Y O 2011 *J. Alloy Compd.* **509** 1711
[43] Parlinski K 2001 *Acta Phys. Pol.* A **100** 767
[44] Li Y, Zeng Z and Lin H 2010 *Chem. Phys. Lett.* **492** 246
[45] Isaev E I, Simak S I, Abrikosov I A, Ahuja R, Vekilov K Yu, Katsnelson M I, Lichtenstein A I and Johansson B 2007 *J. Appl. Phys.* **101** 123519
[46] Koushik B and Charles W M 2007 *Phys. Rev.* B **75** 245205
[47] Peng H, Wang C L, Li J C, Zhang R Z, Wang M X, Wang H C, Sun Y and Sheng M 2010 *J. Electron. Mater.* **40** 620
[48] Li Y, Fan W, Sun H, Cheng X, Li P and Zhao X 2011 *J. Appl. Phys.* **109** 113535
[49] Chu W, Wu Z, Liu W, Saini N L, Bianconi A, Hu T and Xie Y 2006 *Radiat. Phys. Chem.* **75** 2080
[50] Vajeeston P, Ravindran P, Ravi C and Asokamani R 2001 *Phys. Rev.* B **63** 045115
[51] Heid R, Renker B, Schober H, Adelmann P, Ernst D and Bohnen K P 2003 *Phys. Rev.* B **67** 80510
[52] Tütüncü H M, Bagci S and Srivastava G P 2007 *J. Phys.: Condens. Matter* **19** 156207
[53] Soni H R, Gupta S K and Jha P K 2011 *Physica* B **406** 3556
[54] Babu K R, Lingam C B, Auluck S, Tewari S and Vaitheeswaran G 2011 *J. Solid State Chem.* **184** 343
[55] Peng H, Wang C L, Li J C, Zhang R Z, Wang M X, Wang H C, Sun Y and Sheng M 2010 *Phys. Lett.* A **374** 3797
[56] Sanati M, Alberts R C, Lookman T and Saxena A 2011 *Phys. Rev.* B **84** 014116